Speed Up of Near-Field Physical Optics Scattering Calculations by Use of the Sampling Theorem*

Paul W. Cramer and William A. Imbriale
Jet Propulsion Laboratory
California Institute of Technology
4800 Oak Grove Dr., Pasadena, California 91109

Abstract — **Physical optics scattering calculations performed on the NASA Deep Space Network (DSN) 34-meter beam-waveguide antennas at Ka-band requires approximately 12 hours CPU time on a Cray Y-MP2 computer — excessive in terms of resource utilization. The calculations are done two mirrors at a time. The sampling theorem is used to reduce the number of points on the second surface obtained by performing a physical optics integration over the first surface. The number of points required by subsequent physical optics integrations is obtained by interpolation. Time improvements on the order of 2 to 4 were obtained for typical scattering pairs.**

I. INTRODUCTION

The technique discussed here was developed to reduce the time required by physical optics in the computing of the antenna patterns of the 34-m beam-waveguide antennas at the NASA/Jet Propulsion Laboratory's Deep Space Network (DSN). Figure 1 illustrates a typical DSN beam-waveguide (BWG) antenna. With n mirrors, the pairwise analysis must be repeated n-1 times before the final far fields are evaluated, For analysis up to X-band, the available computers could easily handle calculations of such size and complexity. However, with the shift to Ka-band to support future deep space missions, computational times are increased by a factor of about 16.

This paper presents a method to reduce the overall time by a factor of 4 or more for a typical pair of scattering surfaces and by a factor of 2 for the overall antenna system. The sampling theorem coupled with a near-field radial interpolation is used to speed up the physical optics calculations.

The sampling theorem has been previously used for the far-field analysis of reflecting surfaces [1], and a sampling-like technique [2] that allows the use of the FFT (Fast Fourier Transform) algorithm has been used both for the far field of a parabolic reflector and for the Fresnel zone fields of a planar aperture. Both methods [1] and [2] were extended to the near field [3], [4], but were limited to evaluating the fields on a spherical surface of constant radius.

*Manuscript received November 1, 1993. The work described in this paper was performed at the Jet Propulsion Laboratory, California Institute of Technology, under a contract with the National Aeronautics and Space Administration.

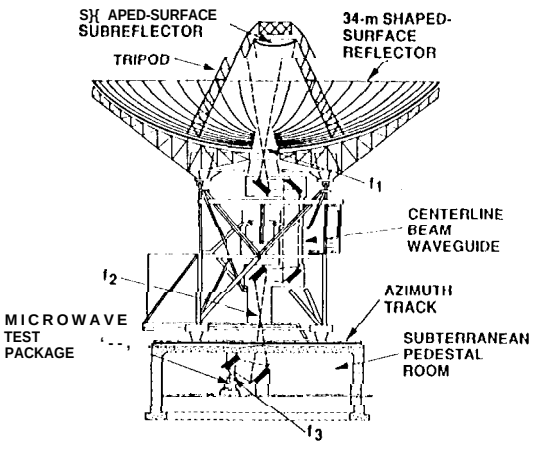

Fig. 1. 34-m BWG antenna.

Evaluating a BWG system requires multiple near-field calculations on arbitrary surfaces. To overcome the existing limitations, the sampling technique has been generalized for arbitrary field point calculations in the near field. Also, since evaluations on multiple surfaces are required, a technique is outlined for developing an equivalent source aperture that defines the geometry required to calculate the optimum sampling parameters.

11. METHOD

The basic method used to analyze the 34-m antennas consisted of performing a physical optics integration over the currents on the various surfaces of the antenna. The form of the physical optics program used here [5] is based upon a discrete approximation of the radiation integral. In this approach, the reflector surface is replaced by a triangular facet representation such that. the surface resembles a geodesic dome. The physical optics currents are assumed to be constant in amplitude and phase over each of the facets so the radiation integral is reduced to a simple summation.

To evaluate the complete antenna, an integration is performed over the currents on the first scattering surface to get the currents on the second surface. Using these new currents on the second surface, the process is repeated, continuing utilization of pairs of surfaces until the complete antenna has been analyzed. The final integration over the main reflector uses the Jacobi-Bessel form of physical optics, which is much faster for calculating far field patterns from large reflectors, but unfortunately not amenable to the use of

the sampling theorem. With the exception of the main reflector, each surface is of comparable size, and if the current resolution in any direction is N, then N* physical optics integrations on the first surface are required for each of the N^2 current points on the second scattering surface. This implies N^4 operations and is the real driver for the computational time.

If the number of points evaluated on the second surface can be reduced significantly and replaced by interpolation to obtain the necessary N* points required by a subsequent physical optics calculation, then the computational time will approach that of N^2 operations on the first surface. The physical optics integral is composed of two basic parts, the current term and the kernel or exponential term. The current term is typically a slowly varying function of position, while the kernel varies rapidly as a function of position and observation point. The approach is to employ the sampling theorem to determine the number of surface points necessary to define the surface currents on the second surface, and then to use an interpolation algorithm to obtain the number of points required by the rapidly varying, but easily evaluated kernel.

A key problem is to define a field sampling function that could be used to determine the sampling frequency. Patterns produced by a uniform distribution should have the highest frequency content and should provide a conservative estimator for the maximum sampling frequency. The pattern distribution from a uniform square source distribution is:

$$E(u) = \mathrm{Sin}(u)/(u).$$

where: $u = 2\pi X_m \sin\theta/\lambda$

X_m = center to edge dimension of the source aperture

θ = angle to a field point on the sampling surface

A = wavelength

If this distribution is evaluated on the sampling surface, then the distance from the surface center to its edge in u, v space is:

$$u_m = 2\pi X_m \mathrm{Sin}\ \theta_m/\lambda$$

where: θ_m = angle to the edge of the sampling surface.

Since the sampling theorem requires sampling at twice the highest frequency, letting

$$B = u_m/2\pi$$

be the sampling frequency, over the full width the number of samples would be:

$$N = 4\, X_m \sin\theta_m/\lambda + 1$$

The Sin(u)/(u) function is based on a far-field derivation. Although it does not provide a rigorous basis for estimating the sampling frequency for sampling surfaces in the near field, it still gives a good estimate for typical source aperture fields. Also, the fields on the sampling surface are not a strictly band-limited function. To account for these limitations, an 18 percent oversampling was used, and (as will be shown later) provides sufficient accuracy.

Since the Sin(u)/(u) field function is defined on a spherical surface, the sampling must also be done on a spherical surface. In addition, the origin of the spherical surface must be at the field function phase center so as to minimize the phase variations over the spherical surface. In addition, the origin must also be at the center of the source aperture. In general there are three problems: First, the reflector surfaces usually are not spherical. Second, the center of the source aperture may not be the phase center of the scattered fields. And third, even if the reflector surface was spherical, the scattered field phase center may not be located at the origin of the spherical reflector. To accommodate non-spherical surfaces or offset phase centers, the surface of interest is enclosed by two spherical surfaces, with the origins of the two surfaces at the phase center of the scattered fields. Figure 2 illustrates the geometry. In the figure are five surfaces: in addition to the sub reflector (source aperture) and the main reflector (ultimate sampling surface), there are the two surfaces enclosing the main reflector, and an equivalent aperture. If the phase center dots not coincide with the center of the source aperture, an equivalent source aperture is constructed at the phase center.

To determine where the phase center should lie, a subset of points are calculated on a spherical surface constructed midway between the two spherical reflectors described above. A phase center location is computed from these points that minimizes the phase pattern variation, in a least squares sense, over the spherical surface, the origin of which coincides with the compute phase center location. A discussion of this technique is beyond the scope of this article; however W. Rusch and P. Potter [6] describe a two-dimensional technique which is the basis of the three-dimensional technique used here. The objective is to minimize

$$\sigma = \sum w_i (kd \cos\gamma_i + c - \Phi_i - \bar{\Delta})^2$$

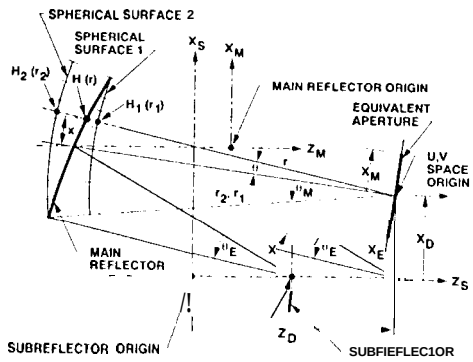

Fig. 2. Interpolation geometry.

where:

w_i	=	phase weight
k	=	propagation constant
d	=	computed vector determining offset to phase center location
γ_i	=	direction to field phase point
c	=	residual phase of pattern relative to phase center
Φ_i	=	phase pattern on spherical surface relative to origin
$\bar{\Delta}$	=	mean of kd cos γ_i + c - Φ_i

The phase center algorithm used is based on far-field approximations, i.e., the distance to the phase center location is small compared to the size and distance to the surface on which the phase is evaluated. This limitation is overcome by iterating the algorithm until the last estimate of the correction to the phase center position is smaller than some specified value.

The equivalent aperture size is estimated to produce a field distribution similar to that on the main reflector. Referring to Figure 2, the equivalent aperture size is:

$$X_m = S_f X_e \text{ Sin } \theta_e / \text{Sin } \theta_m$$

where:

S_f	=	oversampling parameter
X_m	=	center to edge dimension of equivalent aperture
X_e	=	center to edge dimension of source aperture (subreflector)
θ_m	=	angle to edge of sampling surface for equivalent aperture
θ_e	=	angle to edge of sampling surface for source aperture (orthogonal size)

Since a square aperture is used, $Y_m = X_m$. This size is used in the calculation of the number of sample points N. A radius from the center of the equivalent source aperture (phase center) is constructed to the interpolation point on the surface of interest and made to intercept the two spherical surfaces. Interpolated fields are computed on the two spherical surfaces at the intersection points of the radius. The polar interpolation on the two spherical surfaces is expressed as follows:

$$H_{(u,v)} = \sum_{n_u=-N_u/2}^{N_u/2} \sum_{n_v=-N_v/2}^{N_v/2} H_{n_u,n_v} \frac{Sin(u-n_u\pi)}{(u-n_u\pi)} \frac{Sin(v-n_v\pi)}{(v-n_v\pi)}$$

where: u = 27r x $X_m/(\lambda r)$; v = 2π y $Y_m/(\lambda r)$

Thus the two field points H, and H_2 are calculated at r_1 and r_2 respectively on the two surfaces. Next, a radial interpolation is performed between these two points to obtain the interpolated field point on the surface of interest. Since a near-field interpolation is required, terms of the order 1/r and 1/# are used. The appropriate equations are as follows:

$$H = \frac{e^{-jkr}}{4\pi r} (A. + \frac{A_1}{r})$$

where:

$$\text{‹ } ^0 \text{ -} \frac{4\pi}{(r_1 - r_2)} (r_1^2 H_1 e^{-jkr_1} - r_2^2 H_2 e^{-jkr_2})$$

$$A_1 = \frac{4\pi r_1 r_2}{(r_2 - r_1)} (r, H, e^{-jkr_1} - r_2 H_2 e \text{ “k”})$$

This process is repeated until all the currents that are required for subsequent physical optics calculations have been calculated.

III. RESULTS

Figures 3 and 4 show the accuracy of the sampling approach. Figure 3 shows the fields calculated on the

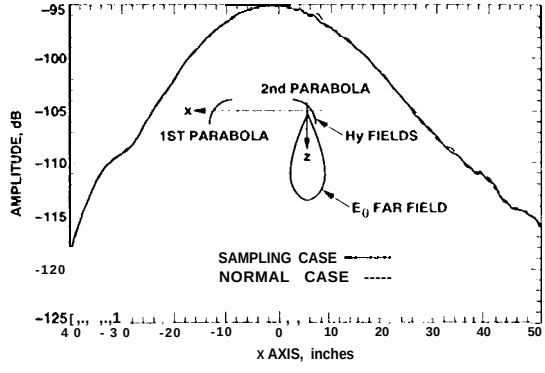

Fig. 3. H_y field on surface of second parabola.

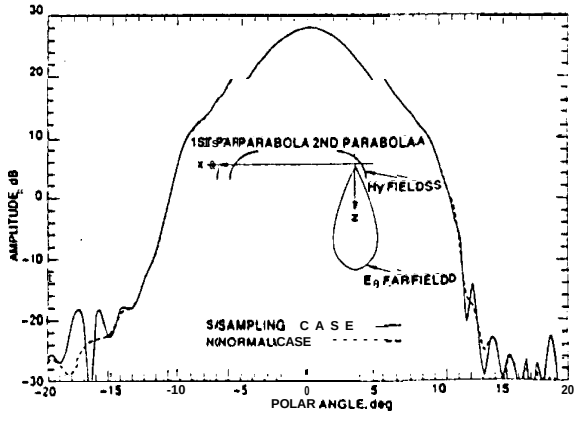

Fig. 4. E-O far-field component, parabola/ parabola, ϕ = O.

sampling surface, one curve where all the points are calculated in the normal manner and a second curve for the case where interpolation is done with a sparse set of sample points. There is a small amount of ripple, less than 0.5 dB, but as seen in the Figure 4, it has a negligible effect on performance. The curves shown in Figure 4 are for the far fields calculated by performing a physical optics integration over the currents on the second parabola (sampling surface). One curve uses currents calculated using the sampling theorem and the other curve is based on the currents being computed using physical optics integration for all current points. As can be seen, the two curves are essentially identical over 40 dB. The differences are primarily in the sidelobe region, However, the sidelobe regions do not illuminate subsequent scattering surfaces and therefore are of no interest in this particular application.

An investigation was made to determine the effect of the size of the oversampling parameter on the accuracy of the computation of the scattered patterns. Figure 5 illustrates the effect of the oversampling parameter for a combination of an ellipse and a parabola. The upper 28 dB of the pattern was truncated to give more resolution to the area most affected by the oversampling parameter. As can be seen, a value of 1.18 is sufficient for a dynamic range of 37 dB. Except for the error at the 37-dB relative level, a value of 1.6 followed the main lobe down to at least the 58-dB relative level. As can be seen, larger oversampling values did not help in the side-lobe region. It is recommended that convergence tests be run for each general application, especially if a smaller value of the oversampling parameter is desired. The effect of increasing the sampling surface beyond the limits of the actual surface by as much as 20 percent was investigated and was found to have very little effect and was not pursued further.

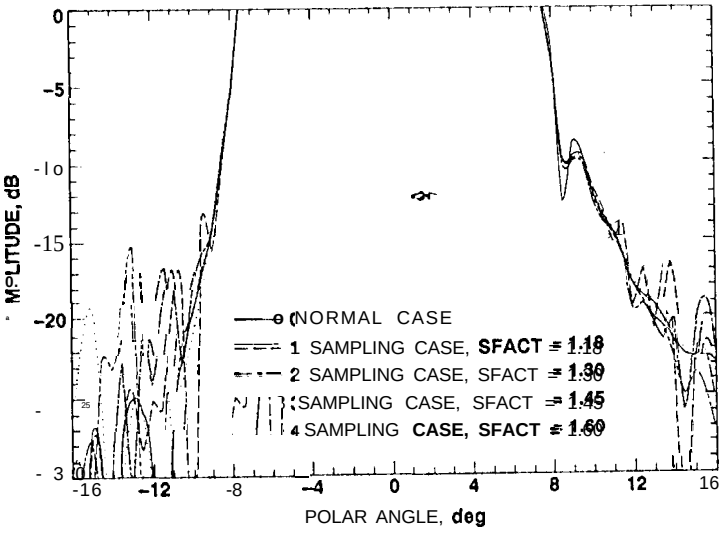

Fig. 5. **E-O far-field component, ellipse/parabola, $\phi = 0$.**

Table 1 is a summary of the time improvement for a calculation on a 34-m beam-waveguide antenna at Ka-band. The results are shown by mirror pairs, the first mirror being the source mirror and the second mirror being the sampling mirror, The difference in time between the first two cases is easily accounted for. The sampling frequency is based on the size of the source aperture and the subtended angle produced by the sampling surface, In the second case the two mirrors are closer together, increasing the subtended angle and in turn requiring a higher sampling frequency. The overall improvement up to and including the subreflector is a factor of 2,73, The sampling theorem was not applied to the main reflector calculation, so an improvement factor of 1.0 was assigned. Including the main reflector, a net improvement of 2.05 was obtained, reducing computation time from 11,55 hours to 5.64 hours.

Table 1. 34-m BWG antenna analysis summary at Ka-band.

GEOMETRY	INTEGRATION POINTS PER AXIS, 1ST/2ND SURFACE	POINTS PER WAVELENGTH	TIME SAMPLING, minutes	TIME NORMAL, minutes	TIME RATIO
ELLIPSE/PARABOLA	340/270	1/1	64.43	2s2.00	4.39
PARABOLA/PARABOLA	270/270	1/1	107.54	181.32	1.69
PARABOLA/SUBREFLECTOR	270/200	1/0.5	328S	94.72	2.88
SUBTOTAL			204.85 (3.41h)	559.04 (9.32h)	2.73
SUBREFLECTOR/MAIN	200/24	0.W-	123.s2	133.82	1.00
TOTAL			33s.s7 (5.64h)	692.86 (11.55h)	2.05

REFERENCES

[1] O.M. Bucci, G. Franceschetti, and C. D'Elia, "Fast Analysis of large antennas: A new computational philosophy, " *IEEE Trans. on Antennas and Propagation, Vol. AP-28, No. 3, May 1980.*

[2] O.M. Bucci, G. Franceschetti, and R. Pierri, "Reflector antennas fields: An exact aperture-like approach, " *IEEE Trans. on Antennas and Propagation, Vol. AP-29, No.* 4, July 1981,

[3] G. D'Elia, G. Leone, R. Pierri, and D. Valentine, "Numerical evaluation of the near field using sampling expansions, " 1982 *APS Symposium, Vol. 1,* pp 241-244.

[4] F. Benici, G. D'Elia, and R. Pierri, "Numerical evaluation of Fresnel-Zone fields by sampling like technique, " 1982 *APS Symposium, Vol. 2,* pp 515-518.

[5] W.A. Imbriale and R. Hodges, "Linear phase approximation in the triangular facet near-field physical optics computer program, " *Applied Computational Electromagnetic Society Journal, Vol. 6, No. 2,* Winter 1991,

[6] W.V.T. Rusch and P. D. Potter, *Analysis of Reflector Antennas,* Academic Press. 1970, pp 145-153.